# iJRASET

# INTERNATIONAL JOURNAL
# FOR RESEARCH

IN APPLIED SCIENCE & ENGINEERING TECHNOLOGY

www.ijraset.com

Call: ◎08813907089 | E-mail ID: ijraset@gmail.com

# Power Quality Disturbances Identification Using Three-band Wavelet Packet Transform

Pashmi N. Kumawat [1], Dinesh K. Verma [2]

[1]Department of Mathematics, Veer Narmad South Gujarat University, Surat, Gujarat, India.

[2]Department of Mathematics, Narmada College of science and commerce, Bharuch , Gujarat,  India.

Abstract: This article proposes the use of three-band Wavelet Packet Transform (i.e. M-band wavelet packet transform with M=3) based technique to recognise the power quality disturbances. The power quality issues such as voltage sag, voltage swell, momentary interruptions, voltage sag along with harmonics, voltage swell along with harmonics, flicker, transient and signals polluted due to presence of harmonics are simulated in MATLAB environment as per IEEE 1159-2009 standards definition. Identification of these power quality problems is carried out using a statistical parameter, Root Mean Square (RMS) of the signal which is computed for each wavelet packet transform coefficient. Analysis is carried out for different magnitudes of disturbances as well as for different time durations.The detailed simulation results are presented to support the feasibility of the present technique.
Keywords: Power quality, Wavelet transform, M-band wavelet packet transform, Three-band wavelet packet transform, RMS

## I. INTRODUCTION

Pollution has been introduced into power systems due to nonlinear loads such as transformers and saturated coils; however, perturbation rate has never reached the current levels [1]. Power Electronics converters, ever more widely used in industrial, commercial and domestic applications, suffer from the problem of drawing non-sinusoidal current and reactive power from the source [2]. So, power quality (PQ) analysis is becoming the most interesting area of research in past several years for characterization [3,4] and classification of events [5]. Poor power quality (PQ) may lead to partial or complete failure of equipment, loss of important data etc. Prior identification of the type and location of disturbances is of foremost importance in modern electric distribution system [6]-[7]. The various types of PQ issues are defined in IEEE standards 1159-2009 in terms of their frequency, magnitude and duration. Perfect evaluation of the electric power quality requires established and standard indices to quantify the effect of different power quality disturbances [8]. The acceptable PQ indices should be able to show the amount of deviation from the desired pure power supply [9]-[11]. Moreover, the detection and localization of the disturbances lead to know the causes and sources of disturbances [12].

The fast detection of PQ disturbance is becoming an important factor in deregulated market [13]. Different signal processing techniques have been used in order to detect and identify the disturbances. The Fourier Transform is suitable to analyze stationary signals but not suitable for non-stationary signals such as the transient signals [14].To resolve this, the short time fourier transform (STFT) divides the signal into small segments, where these signal segments can be assumed to be stationary [15]. Wavelet transform is more suitable than STFT as STFT possesses fixed window property [16]. Popular extensions to the wavelet transform are the wavelet packet transform (WPT) and the M-band wavelet transform [17]. If there are high frequency signals with relatively narrow bandwidth (like a long RF pulse), the decomposition is not well suited [18]. In order to overcome this problem M-band orthonormal wavelet bases have been constructed recently by several authors [19], [20] as a direct generalization of the two-band wavelets of Daubechies [21].M-band WPT is the direct generalisation of conventional two-band WPT [22]. In contrast to M-band wavelet decompositions, M-band wavelet packets allow more flexible time frequency tiling.

Previously the analysis of PQ disturbances was done using conventional two-band WPT [14]. The main objective of this paper is to propose a method for the detection and analysis of PQ disturbances using three-band WPT.

## II. M-BAND WAVELET PACKET TRANSFORM

The mathematical back ground of M-band wavelets enables the construction of M-band WPT similar to two-band WPT. Let $h_0 \in \mathbb{R}^N \to l^1(\mathbb{Z})$ be a unitary M-band scaling filter of finite length N, i.e.

$$\sum_{k=0}^{N-1} h_0(k) = \sqrt{M} \qquad (1)$$

$$\forall\, l \in \mathbb{Z} : \sum_{k=0}^{N-1} h_0(k)\, h_0(k + Ml) = \delta(l) \qquad (2)$$

Then the M-band dilation equation [18]

$$\psi_0(t) = \sqrt{M} \sum_{k=0}^{N-1} h_0(k)\, \psi_0\,(Mt - k) \tag{3}$$

Has a unique solution $\psi_0 \in L^2(\mathbb{R}) \cap L^1(\mathbb{R})$.

For a given $h_0$ sequence of unitary wavelet filters $h_1, \ldots, h_{M-1}$ of length $N$ is chosen, i.e., a sequence of filters $(h_0, h_1, \ldots, h_{M-1})$ forming a unitary M-band filter bank.

Then, for $1 \leq i \leq M$,

$$\psi_i(t) := \sqrt{M} \sum_{k=0}^{N-1} h_i(k)\, \psi_0\,(Mt - k) \tag{4}$$

Defines $M - 1$ wavelets $\psi_1, \psi_2, \ldots, \psi_{M-1}$ whose dilates and translates form a wavelet tight frame for $L^2(\mathbb{R})$ [18]. Now recursively define M-band wavelet packet functions by

$$W_0 := \psi_0, \ldots, W_{M-1} := \psi_{M-1} \tag{5}$$

Further, for $n \epsilon \mathrm{N}$ and $0 \leq j < M$, $W_{M_{n+j}}(t) := \sqrt{M} \sum_{k \epsilon \mathbb{Z}} h_j(k) W_n (Mt - k)$. Defining the dilation operator $\delta_M f(.) := \sqrt{M} f(M)$.

The M - band WPT produces large number of sub bands which improve the accuracy and it is required for good quality segmentation. Fig. 1 shows the decomposition tree of M-band WPT with M=3 up to decomposition level 2 for 1-D signal. At level (0,0) the sampled signal is passed through first level of three-band biorthogonal linear phase wavelet filters in order to get one approximate coefficient and two detailed coefficients i.e. (1,0) ,(1,1) and (1,2) resp. At the next level approximate as well as both detail coefficients will again pass through three-band biorthogonal linear phase wavelet filters. This process is continued till the desired level of decomposition is achieved.
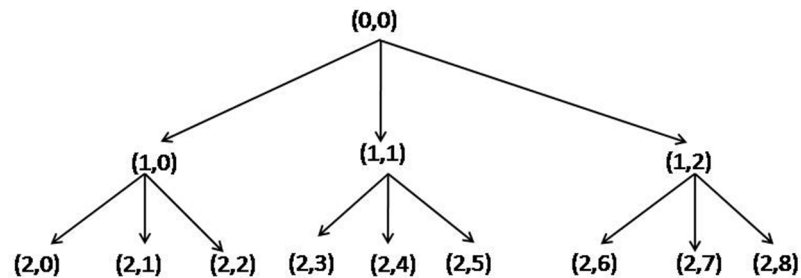


Fig. 1 Two Level decomposition of 1-D signal using three-band WPT

Ideal $M$-band filter bank with $M > 2$ subbands is the extension of the two band filter bank which improves the frequency resolution [23]. In M channel filter bank the bandwidth of the filter bank is divided into M bands [24] as shown in Fig. 2.
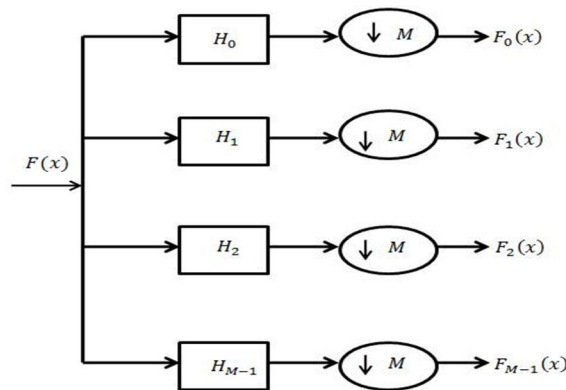


Fig.2  M-channel analysis filter bank

Thus, WPT analyses both high and low frequency contents of the signal. In addition to this, M-band WPT generates more number of sub bands as compare to conventional two-band WPT. This makes M-band WPT a strong contender for finer PQ analysis.

### III. MODELLING AND COMPUTATION OF PQ DISTURBANCES

Power quality disturbances such as voltage sag, voltage swell, momentary interruptions, voltage sag plus harmonics, voltage swell plus harmonics, flicker, transients and 2 different patterns of harmonics are generated with variation in magnitude and time as per IEEE 1159-2009 standards. PQ disturbances are processed with three-Band WPT up to decomposition level two using three-band biorthogonal linear phase wavelet filters. Modeling equations of the pure (i.e. ideal) signal and PQ Disturbances studied are given in Table 1.

TABLE I
MODELLING EQUATIONS OF POWER QUALITY DISTURBANCES

| PQ Disturbance | Modelling Equation |
|---|---|
| Pure (No disturbance) | $h(t) = \sin \omega t$ |
| Voltage Sag | $h(t) = \left[1 - \alpha\big(u(t - t_1) - u(t - t_2)\big)\right] \sin(\omega t)$ |
| Voltage Swell | $h(t) = \left[1 + \alpha\big(u(t - t_1) - u(t - t_2)\big)\right] \sin(\omega t)$ |
| Momentary interruption | $h(t) = \left[1 - \alpha\big(u(t - t_1) - u(t - t_2)\big)\right] \sin(\omega t) , \; \alpha = 0.99$ |
| Voltage sag plus harmonics | $h(t) = \left[1 - \alpha\big(u(t - t_1) - u(t - t_2)\big)\right](\alpha_1 \sin(\omega t) + \alpha_3 \sin(3\omega t) + \alpha_5 \sin(5\omega t))$ |
| Voltage swell plus harmonics | $h(t) = \left[1 + \alpha\big(u(t - t_1) - u(t - t_2)\big)\right](\alpha_1 \sin(\omega t) + \alpha_3 \sin(3\omega t) + \alpha_5 \sin(5\omega t))$ |
| Flicker | $h(t) = [1 + \alpha \sin(2\pi\beta t)] \sin(\omega t)$ |
| Transient | $h(t) = \sin(\omega t) + \alpha \exp(-(t - t_1)\tau)\big(u(t - t_1) - u(t - t_2)\big) \sin(2\pi f_n t)$ |
| Harmonics pattern 1 | $h(t) = \alpha_1 \sin(\omega t) + \alpha_3 \sin(3\omega t) + \alpha_5 \sin(5\omega t) + \alpha_7 \sin(7\omega t) + \alpha_9 \sin(9\omega t)$ |
| Harmonics pattern 2 | $h(t) = \alpha_1 \sin(\omega t) + \alpha_2 \sin(2\omega t) + \alpha_3 \sin(3\omega t) + \alpha_4 \sin(4\omega t) + \alpha_5 \sin(5\omega t)$ $+ \alpha_6 \sin(6\omega t) + \alpha_7 \sin(7\omega t)$ $+ \alpha_8 \sin(8\omega t) + \alpha_9 \sin(9\omega t) + \alpha_{10} \sin(10\omega t)$ |

Fig. 3(a) , 3(b) and 3(c) show voltage sag, voltage swell and momentary interruption respectively generated with the time period of 2 seconds. Fig. 3(d) shows transient with time period in milliseconds.
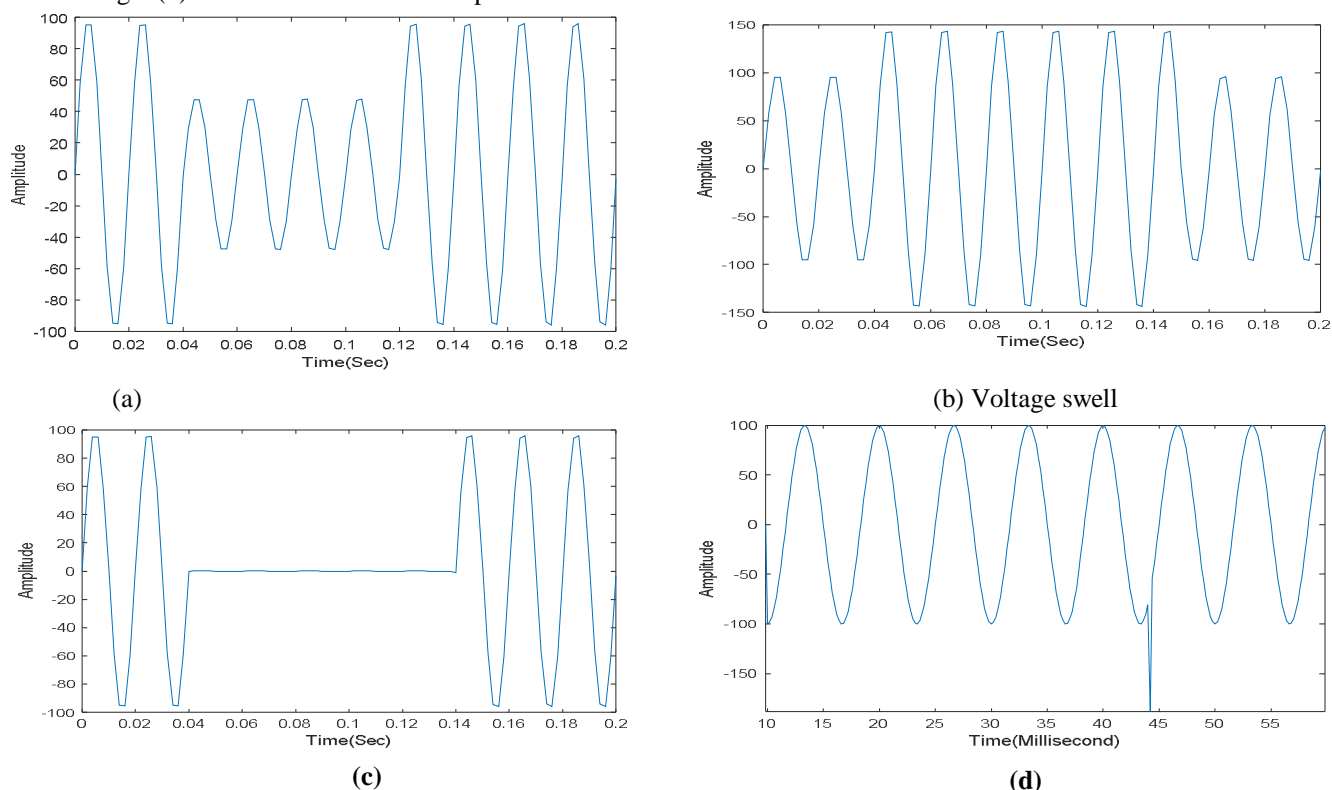


(a)

(b) Voltage swell

(c)

(d)

Fig. 3. Simulated PQ disturbances (a) Voltage sag (b) Voltage swell (c) Momentary Interruption (d) Transient

Fig. 4(a) and (b) show harmonics along with 50% voltage swell and harmonics with 50% voltage sag for 5 cycle duration respectively.Fig. 4 (c) and (d) show signals polluted due to presence of harmonics. Flickers for time duration of 0.2 seconds are given in Fig. 4 (d).
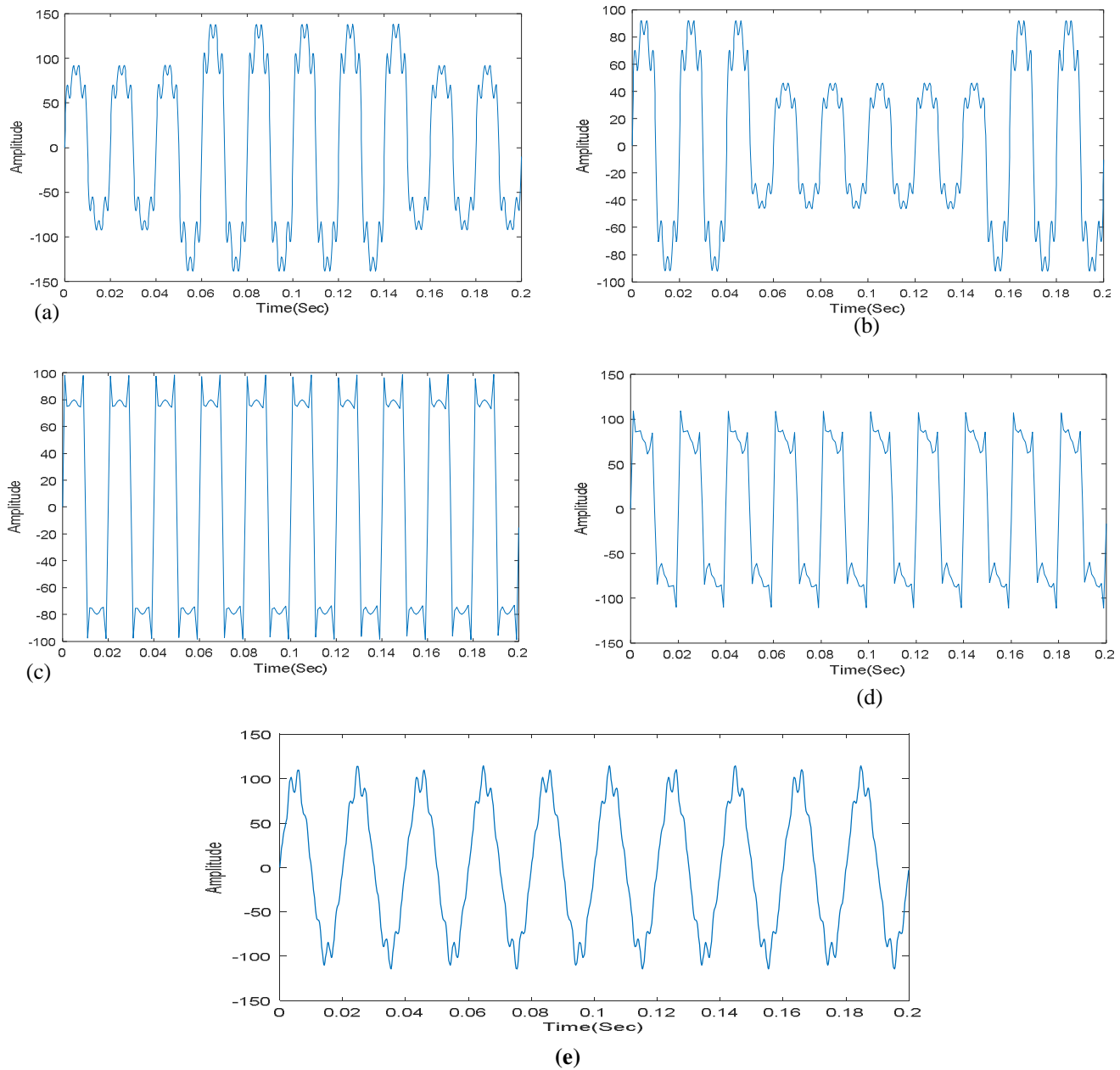


Fig. 4. Simulated PQ disturbances (a) Voltage swell with harmonics (b) Voltage sag with harmonics (c) Harmonics pattern 1 (d) Harmonics pattern 2 (e) Flicker

## IV. SIMULATION RESULTS AND DISCUSSION

A statistical parameter RMS$_{wpt}$ based on the RMS value of the three-band WPT co-efficient is computed for each decomposition coefficient (i,j) and for all the PQ disturbances as:

$$RMS_{wpt} = \sqrt{\frac{\sum_{k=1}^{n}(x_k)^2}{n}} \qquad (6)$$

Where,   n=length of the (i, j)th three-band WPT decomposition coefficient.

Fig. 5 (a)-(b) show the plot of RMS$_{wpt}$ of voltage sag to its three-band WPT decomposition coefficients with variation in sag magnitude and cycle variation respectively. Plots also show the behaviour of the RMS$_{wpt}$ for pure signal. It can be observed that the value of statistical parameter RMS$_{wpt}$ decreases from the value of the same parameter calculated for pure signal as the magnitude or cycle duration of disturbance increases especially for the decompositions belonging to the left hand side of the decomposition tree in Fig. 1 (i.e. for lower frequency bands).
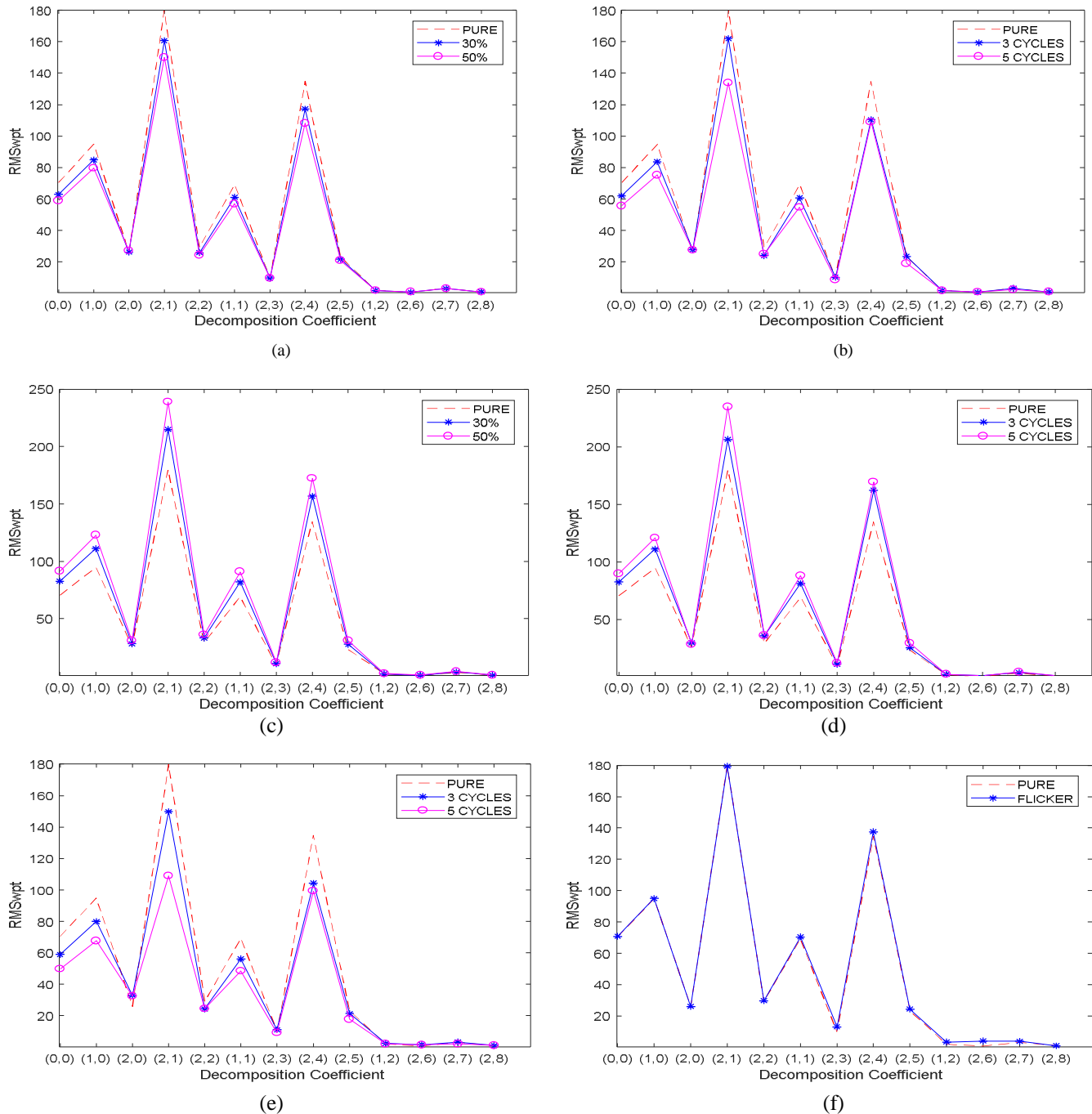


Fig. 5 RMS$_{wpt}$ analysis of PQ disturbances for (a) Voltage sag with variation in magnitude (b) voltage sag with variation in duration  (c) Voltage swell with variation in magnitude (d) Voltage swell with variation in duration (e) Momentary interruption of 3 and 5 cycles (f) Flickers

It can be observed from Fig. 5 (c) and (d) that in case of voltage swell, value of RMS$_{wpt}$ increases from pure with increase in magnitude or cycle duration of the disturbance. Similar plot for momentary interruption with variation in cycle duration is given in Fig. 5 (e). In this case the behaviour of the RMS$_{wpt}$ is same as voltage sag. Fig. 5 (f) indicates that for flicker the values are slightly higher than that of pure signal. Fig. 6 (a) and (b) show that for voltage sag with harmonics the value of RMS$_{wpt}$ decreases from pure for the lower frequency band whereas in case of voltage swell plus harmonics it increases from pure signal. From Fig. 6 (c) and (d) it can be observed that for both the patterns of harmonically polluted signals, RMS$_{wpt}$ is showing higher values than pure signal. The graphs show major change from pure signal at decomposition coefficient (2, 0).
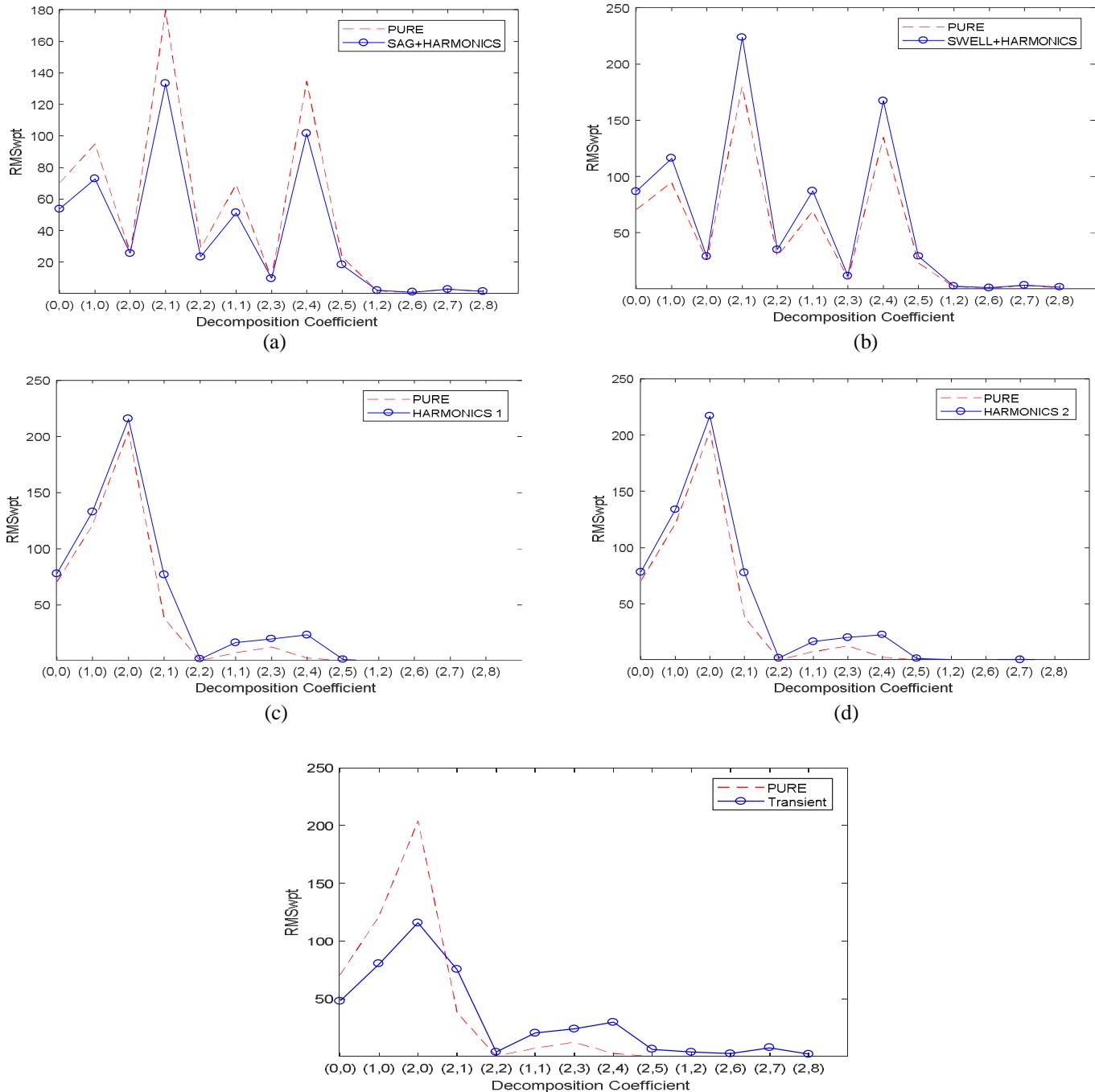


Fig. 6 RMS$_{wpt}$ analysis of PQ disturbances for (a) Voltage sag with harmonics (b) Voltage sswell with harmonics (c) Harmonics pattern 1(d) Harmonics pattern 2 (e) Transient

Fig. 6(e) shows that in case of transient, value of statistical parameter $RMS_{wpt}$ decreases drastically from pure at decomposition coefficient (2,0).Fig. 5 and Fig. 6 show that there are prominent changes in the values of RMSwpt at decomposition coefficient (2,1) and (2,4) for voltage sag, voltage swell, momentary interruption and also for flicker. Detailed analysis of $RMS_{wpt}$ at these two decomposition coefficients is presented in the tabular form below. On comparing these results with the results obtained by conventional two-band WPT based technique [14], it can be observed that the three-band WPT is giving equally accurate results at lower decomposition level with more number of subbands i.e. three-band WPT is giving finer analysis with less computational complexity.

Analysis of $RMS_{wpt}$ value for decomposition coefficients (2,1) and (2,4) for voltage sag with variation in magnitude (keeping constant duration) and with variation in time duration (keeping constant magnitude) is given in Table 2. Similar analysis for voltage swell is given in Table 3.

It can be observed from Table 2 that as magnitude of voltage sag increases the $RMS_{wpt}$ decreases linearly for both the decomposition coefficients. Also as time duration of voltage sag with constant magnitude increases, the values of $RMS_{wpt}$ at both the decomposition coefficients (2, 1) and (2, 4) decreases as compared to pure signal result.

TABLE II

ANALYSIS OF $RMS_{wpt}$ AT COEFFICIENT (2,1) AND $RMS_{wpt}$ AT COEFFICIENT (2,4) FOR VOLTAGE SAG MAGNITUDE VARIATION AND TIME DURATION VARIATION

| Sr.No. | Sag Magnitude (%) | Duration (Cycles) | $RMS_{wpt}$ at (2,1) | $RMS_{wpt}$ at (2,4) |
|---|---|---|---|---|
| 1 | 0 | 4 | 179.86 | 134.72 |
| 2 | 30 | 4 | 160.63 | 117.24 |
| 3 | 50 | 4 | 149.99 | 108.16 |
| 4 | 50 | 3 | 162.06 | 110.38 |
| 5 | 50 | 5 | 133.88 | 108.92 |

Table 3 shows that as magnitude of voltage swell increases, the $RMS_{wpt}$ increases linearly for both the decomposition coefficients. Also as time duration of voltage swell with constant magnitude increases the values of $RMS_{wpt}$ at (2, 1) and (2, 4) increase.

TABLE III

ANALYSIS OF $RMS_{wpt}$ AT COEFFICIENT (2,1) AND $RMS_{wpt}$ AT COEFFICIENT (2,4) FOR VOLTAGE SWELL MAGNITUDE VARIATION AND TIME DURATION VARIATION

| Sr.No. | Swell Magnitude (%) | Duration (Cycles) | $RMS_{wpt}$ at (2,1) | $RMS_{wpt}$ at (2,4) |
|---|---|---|---|---|
| 1 | 0 | 4 | 179.86 | 134.72 |
| 2 | 30 | 4 | 214.87 | 156.72 |
| 3 | 50 | 4 | 239.09 | 172.47 |
| 4 | 50 | 3 | 206.39 | 162.26 |
| 5 | 50 | 5 | 234.84 | 169.52 |

Results of similar analysis for Momentary interruptions with variation in duration are given in Table 4.With increase in time duration the value of $RMS_{wpt}$ decreases from pure for both the decomposition coefficients.

TABLE IV

$RMS_{wpt}$ ANALYSIS FOR MOMENTARY INTERRUPTION WITH VARIATION IN TIME DURATION

| Sr. No. | Duration (Cycles) | $RMS_{wpt}$ at (2,1) | $RMS_{wpt}$ at (2,4) |
|---|---|---|---|
| 1 | 0 | 179.86 | 134.72 |
| 2 | 3 | 149.87 | 104.31 |
| 3 | 5 | 108.97 | 99.40 |

Table 5 shows the RMS$_{wpt}$ values at each WPT coefficient upto decomposition level 2 (Fig. 1) for voltage sag with harmonics and voltage swell with harmonics. The same table also contains the results for pure signal, flicker and transient. Here prominent change is observed at decomposition coefficient (2, 1) for pure signal as well as for voltage sag with harmonics, voltage swell with harmonics and flicker. In case of transient, Table 5 shows that major change is noticed at decomposition coefficient (2, 0) which is low frequency coefficient. It is observed that for lower frequency coefficients the value of RMS$_{wpt}$ is less than the value of RMS$_{wpt}$ for pure signal. But moving towards higher frequency coefficients (i.e. coefficients to the right of (2, 2) in the graph) the value of RMS$_{wpt}$ is having values higher than that of pure signal.

TABLE V
RMS$_{wpt}$ VALUES FOR PQ DISTURBANCES WITH FIXED MAGNITUDE AND TIME DURATION

| Decomposition coefficient | RMS$_{wpt}$ at (2,1) | | | | |
|---|---|---|---|---|---|
| | Pure | Voltage Sag with harmonic | Voltage Swell With harmonic | Flicker | Transient |
| (0,0) | 70.38 | 53.75 | 86.65 | 70.78 | 48.15 |
| (1,0) | 94.81 | 72.83 | 116.29 | 94.97 | 80.49 |
| (2,0) | 25.92 | 25.62 | 28.83 | 25.98 | 115.81 |
| (2,1) | 179.86 | 133.27 | 223.69 | 179.40 | 75.58 |
| (2,2) | 29.13 | 23.22 | 35.02 | 29.68 | 4.03 |
| (1,1) | 69.17 | 51.29 | 87.03 | 70.40 | 20.47 |
| (2,3) | 9.78 | 9.69 | 11.68 | 12.95 | 23.98 |
| (2,4) | 134.72 | 101.55 | 167.22 | 137.59 | 29.77 |
| (2,5) | 23.22 | 18.27 | 29.21 | 24.37 | 6.42 |
| (1,2) | 1.85 | 2.12 | 2.64 | 3.27 | 4.01 |
| (2,6) | 0.57 | 0.94 | 1.01 | 3.98 | 2.73 |
| (2,7) | 3.15 | 2.73 | 3.41 | 3.78 | 7.80 |
| (2,8) | 0.85 | 1.41 | 1.80 | 0.85 | 2.22 |

Similar analysis for Harmonics pattern 1 and pattern 2 is given in Table 6. The prominent change is noticed at decomposition coefficient (2, 0) which is lower frequency coefficient.

TABLE VI
ANALYSIS OF RMS$_{WPT}$ VALUES FOR HARMONICS PATTERN 1 AND PATTERN 2

| Decomposition coefficient | RMSwpt for | | |
|---|---|---|---|
| | Pure | Harmonics Pattern 1 | Harmonics Pattern 2 |
| (0,0) | 70.69 | 77.76 | 78.29 |
| (1,0) | 121.52 | 132.87 | 133.79 |
| (2,0) | 204.12 | 215.59 | 217.04 |
| (2,1) | 38.16 | 76.73 | 77.64 |
| (2,2) | 0.41 | 1.99 | 1.89 |
| (1,1) | 7.46 | 16.50 | 16.47 |
| (2,3) | 12.48 | 19.82 | 20.07 |
| (2,4) | 2.72 | 23.16 | 22.57 |
| (2,5) | 0.21 | 1.51 | 1.50 |
| (1,2) | 0.04 | 0.28 | 0.28 |
| (2,6) | 0.05 | 0.23 | 0.23 |
| (2,7) | 0.06 | 0.51 | 0.52 |
| (2,8) | 0.02 | 0.08 | 0.08 |

## V. CONCLUSION

In this paper, a new technique base on three-band wavelet packet transform is proposed for identification of PQ disturbances. Simulated PQ disturbances like voltage sag, voltage swell, momentary interruptions, voltage sag along with harmonics, voltage swell along with harmonics, flicker, transient, and signals polluted due to presence of harmonics are decomposed using three-band WPT up to decomposition level 2.The statistical parameter RMS value of the signal is used for the analysis of the disturbances. Performance of the proposed method has been evaluated for variation in the magnitude and duration of the disturbances like voltage sag, voltage swell and momentary interruptions. From the observations we can conclude the following :

A. The statistical parameter used is showing linear trend which can be considered as a firm reason for reliability of the proposed method for identification and classification of PQ disturbances.

B. Three-band WPT generates more number of subbands than conventional two band WPT which results in finer analysis of the signal.

C. Moreover, three-band WPT is giving equally accurate results as conventional two-band WPT at lower decomposition level which reduces the computational complexity. Thus three-band WPT gives finer analysis of the signal with less computational complexity.

## REFERENCES

[1]    M. M. Morcos and J. C. Gomez, " Electric power quality-the strong connection with power electronics," IEEE Power and Energy Magazine , vol. 99, pp. 18-25, 2003.

[2]    N. Zaveri and T. Zaveri, "Performance of an improved instantaneous current component theory for power quality improvement under non-ideal source voltage conditions, " in *Proc.* International Seminar on Renewable Energy and Sustainable Development, 2015,  p.157.

[3]    S. H. Jaramillo, G. T. Heydt and E. O'Neill-Carrillo, "Power quality indices for aperiodic voltages and currents," IEEE Transactions on Power Delivery 2000; vol. 15(2), pp. 784–90, 2000.

[4]    S. R. Shaw, C. R. Laughman, S. B. Leeb and R. F. Lepard, "A power quality prediction system," IEEE Transactions on Industrial Electronics, Vol. 47(3), pp. 511–517, 2000.

[5]    J. Barros and E. Perez, "Automatic detection and analysis of voltage events in power systems," IEEE Transactions on Instrumentation & Measurement, vol. 55(5),  pp. 1487–1493, 2006.

[6]    IEEE recommended practices and requirements for harmonic control in electrical power quality IEEE std. 519-1992.

[7]    IEEE recommended practice for monitoring electric power quality IEEE std. 1159-2009.

[8]    W. G.  Morsi and M. E. El-Hawaryb, " Novel power quality indices based on wavelet packet transform for non-stationary sinusoidal and non-sinusoidal disturbances," Electric Power Systems Research, vol. 80(7), pp. 753–759, 2010.

[9]    Y. Shin, E. Powers, M. Grady and A. Arapostathis, " Power quality indices for transient disturbances," IEEE Transaction on Power Delivery, vol. 21(1), pp. 253–261, 2006.

[10]   C. A. Naik; and P. Kundu, " Power quality index based on discrete wavelet transform," International Journal of Electrical Power &Energy Systems, vol. 53, pp. 994-1002, 2013.

[11]   P. Kumawat, N. Zaveri and D. K. Verma, "Analysis of Power Quality Disturbances usingz M-band Wavelet Packet Transform," in *Proc.* International Conference on Signal Processing and Communication, 2017, p. 364.

[12]   A. M. Gaouda, M. M. A. Salama, M. R. Sultan and A. Y. Chikhani, "Power quality detection and classification using wavelet-multiresolution signal decomposition," IEEE Transactions on Power Delivery, vol. 14(4), pp.1469 – 1476, 1999.

[13]   S. Upadhyaya and S. Mohanty, "Power Quality disturbance detection using Wavelet based signal processing," in *Proc.*  Annual IEEE India Conference (INDICON), 2013, p.1.

[14]   C. A. Naik and P. Kundu, "Wavelet packet transform based parameter for the analysis of short duration power quality disturbances," IFAC-PapersOnLine, vol. 48, pp. 485-489, 2015.

[15]   R. Gao, R. and R. Yan, From Fourier Transform to Wavelet Transform: A Historical Perspective, Springer, 2010.

[16]   B. K. Panigrahi and V. R. Pandi, " Optimal feature selection for classification of power quality disturbances using wavelet packet-based fuzzy K-nearest neighbour," IET Generation, Transmission and Distribution, vol. 3(3), pp. 296–306, 2009.

[17]   F. Kurth and M. Clausen, " Filter Bank Tree and M-Band Wavelet Packet Algorithms in Audio Signal Processing," IEEE Trans. on Signal Processing, vol. 47(2), pp. 549- 554, 1999.

[18]   P. Steffen, P. N. Heller, R. A. Gopinath and C. S. Burrus, "Theory of regular m-band wavelet bases," IEEE Transactions on Signal Processing, vo. 41(12), pp. 3497-3511, 1993.

[19]   P. Heller, H. W. Resnikoff and R. O. Wells, " Wavelet matrices and the representation of discrete functions. In: C. K. Chui (ed.). Wavelets: A Tutorial in Theory and Applications. New York: Academic Press, Boca Raton, p. 15-50, 1992.

[20]   H. Zou and A. H. Tewfik, "Discrete orthogonal M-band wavelet decompositions," in *Proc.* of IEEE International Conference on Acoustics, Speech, and Signal Processing, 1992, p. 605.

[21]   I. Daubechies, " Orthonormal bases of compactly supported wavelets," Commun. on Pure Appl. Math., vol. 41, pp. 909-996, 1988.

[22]   C. S. Burrus, R. A. Gopinath and H. Guo,  Introduction To Wavelets And Wavelet Transforms: A Primer , Pearson publication, pp. 98-147, 1998.

[23]   D. Bhati, M. Sharma, R. B. Pachori and V. M. Gadre "Time–frequency localized three-band biorthogonal wavelet filter bank using semidefinite relaxation and nonlinear least squares with epileptic seizure EEG signal classification," Digital Signal Processing, vol. 62, pp. 259-273, 2017.

[24]   S. Bharkad and M. Kokare, "Fingerprint Matching Using M Band Wavelet Transform,". in *Proc.* IEEE-International Conference On Advances In Engineering, Science And Management, 2012, p. 26-32.

# INTERNATIONAL JOURNAL FOR RESEARCH

IN APPLIED SCIENCE & ENGINEERING TECHNOLOGY

Call : 08813907089 ⓒ (24*7 Support on Whatsapp)